

Research

Flavokawain A suppresses the malignant progression of neuroblastoma in vitro depending on inactivation of ERK/VEGF/MMPs signaling pathway

Mengyao Dong¹ · Gaiqin Li² · Geng Geng³ · Ming Ming³ · Yongtao Xu³

Received: 16 April 2024 / Accepted: 11 November 2024

Published online: 19 November 2024

© The Author(s) 2024 [OPEN](#)

Abstract

Background Neuroblastoma (NB), the most common extracranial solid tumor in children, is featured by high malignancy and poor prognosis. Flavokawain A (FKA), a novel chalcone isolated from the roots of the kava plant, has been identified to exert the tumor-inhibiting properties in various cancers. The present study was formulated to tell about the anticarcinogenic effects of FKA against NB and to thoroughly elucidate the intrinsic molecular mechanisms.

Methods In this work, for functional experiments, SK-N-SH cells were treated with various concentrations (0, 12.5, 25, 50 μ M) of FKA in order to expound the tumor-inhibiting functions of FKA on proliferative ability, clone-forming ability, apoptosis, cell cycle arrest, migratory ability, invasive ability, EMT and in vitro angiogenesis of NB cells. Moreover, to probe into the intrinsic molecular mechanisms underlying the tumor-inhibiting functions of FKA in NB cells, FKA-treated SK-N-SH cells were co-treated with ERK activator LM22B-10 for rescue experiments.

Results In our current work, it was verified that FKA treatment suppressed the proliferative and clone-forming abilities of NB cells, facilitated NB cell apoptosis, arrested NB cell cycle as well as inhibited NB cell migration, invasion, EMT and in vitro angiogenesis in a dose-dependent manner. What's more, molecular docking predicted the compound-protein interaction between FKA and ERK and biotin pull-down assay validated the binding of FKA to ERK. FKA targeted on ERK and acted as an inhibitor of ERK to inactivate ERK/VEGF/MMPs signaling pathway. Treatment with ERK activator LM22B-10 partially abolished the tumor-inhibiting functions of FKA in NB.

Conclusion Overall, FKA may suppress the malignant behaviors of NB cells depending on inactivation of ERK/VEGF/MMPs signaling pathway.

Keywords Flavokawain A · ERK/VEGF/MMPs pathway · Neuroblastoma

1 Introduction

Neuroblastoma (NB), the most common pediatric solid tumor, is featured by heterogeneity, high malignancy, poor prognosis and easy metastasis [1]. Accompanied by the continuous development of anti-tumor therapy, the survival rate of patients with low and intermediate-risk NB has improved substantially through comprehensive treatment

✉ Yongtao Xu, Xuyongtao850923@163.com | ¹Department of Pediatrics, The Affiliated Taian City Central Hospital of Qingdao University, Taian 271000, Shandong Province, People's Republic of China. ²Department of Gastroenterology, The Affiliated Taian City Central Hospital of Qingdao University, Taian 271000, Shandong Province, People's Republic of China. ³Department of Pediatric Surgery, The Affiliated Taian City Central Hospital of Qingdao University, No.29 Longtan Road, Taishan District, Taian 271000, Shandong Province, People's Republic of China.



such as surgery, radiotherapy, chemotherapy and immunotherapy [2]. In contrast, patients with high-risk NB have a low survival probability, suffering from widespread metastasis and late recurrence [3]. Therefore, exploration of potential biomarkers for early diagnosis and effective therapeutic strategies for NB is in urgent need.

Flavokawain A (FKA) is a novel chalcone isolated from the roots of Kava (*Piper methysticum* Forst) [4]. Notably, FKA has been demonstrated to exert anticarcinogenic effects against various cancers including bladder cancer, prostate cancer, lung cancer, colon cancer, breast cancer and hepatocellular carcinoma [5–10]. Literature reports that FKA can suppress the vasculogenic mimicry of hepatocellular carcinoma by inhibiting CXCL12-mediated EMT [10]. FKA can impair the viability and induce the apoptosis of bladder cancer cells by inhibiting PRMT5 [5]. FKA can reduce the tumor-initiating properties and stemness of prostate cancer [6]. FKA can dose-dependently inhibit the proliferation and promote the apoptosis of paclitaxel-resistant lung cancer cells [7]. FKA can reduce colon cancer cell viability in a dose-dependent manner [8]. FKA can facilitate apoptosis through the intrinsic mitochondrial pathway to restrain the metastatic process in breast cancer cell lines [9]. As a consequence, FKA may serve as a promising candidate in the development of novel anti-cancer drugs for a series of malignant tumors. However, to date, the anticarcinogenic effects of FKA on NB process remains unclear till now.

In the present study, tumor-inhibiting properties of FKA were investigated from these aspects: proliferative ability, clone-forming ability, apoptosis, cell cycle arrest, migratory ability, invasive ability and EMT of NB cells. Moreover, the intrinsic molecular mechanisms underlying the tumor-inhibiting functions of FKA in NB were thoroughly elucidated.

2 Materials and methods

2.1 Cell culture

Human NB cell line (SK-N-SH) and human umbilical vein endothelial cells (HUVECs) purchased from iCell Bioscience (Shanghai, China) were cultured in DMEM (Gibco, CA, USA) supplemented with 10% FBS and 1% penicillin–streptomycin at 37 °C in a humidified incubator containing 5% CO₂.

2.2 Cell treatment

Reagents FKA of ≥ 99% purity (Sigma-Aldrich, MO, USA) was dissolved in dimethyl sulfoxide (DMSO) to form the stock solution. To investigate the specific effects of FKA on the malignant behaviors of NB cells, SK-N-SH cells were treated with 0, 12.5, 25 or 50 μM FKA for 48 h [11].

To explore the intrinsic molecular mechanisms underlying the anticarcinogenic effects of FKA against NB, SK-N-SH cells were treated with 50 μM FKA and/or ERK activator LM22B-10 (5 mmol/L, Sigma-Aldrich, MO, USA) [12].

2.3 Cell counting kit-8 (CCK-8) assay

CCK-8 assay was adopted to detect cell viability. Cells (5×10^3 cells/well) in 96-well plates were subjected to the designed treatment and then 10 μl CCK-8 reagent was added to each well for additional 4 h incubation. The optical density (OD) at 450 nm was measured using a microplate reader.

2.4 Colony formation assay

Colony formation assay was adopted to detect cell colony-forming ability. SK-N-SH cells in the exponential phase of growth were digested, re-suspended in complete medium and then seeded at a density of 500 cells/well into 6-well plates. After 14-day incubation, colonies were fixed with 4% paraformaldehyde and stained with 0.1% crystal violet. Images of visible colonies were photographed under a light microscope. Colonies consisted of ≥ 50 cells.

2.5 Flow cytometry analysis

SK-N-SH cells were trypsinized, collected by centrifugation, resuspended in $1 \times$ Binding Buffer, doubly stained with Annexin V-FITC and PI (Beyotime, Shanghai, China) for 15 min at room temperature in the dark and then subjected to flow cytometry (BD Biosciences, CA, USA) for analysis of cell apoptosis.

SK-N-SH cells were harvested, fixed overnight in 70% ethanol at 4 °C, washed with PBS, stained with PI/RNase Staining Buffer for 30 min at room temperature in the dark and then subjected to flow cytometry for analysis of cell cycle distributions.

2.6 Wound healing assay

Wound healing assay was adopted to detect cell migratory capability. SK-N-SH cells (1×10^5 cells/well) in 6-well plates were grown to 95% confluence. A wound was created by scratching the monolayer of cells with a sterile 200- μ l pipette tip. Afterwards, cells were cultured in fresh serum-free DMEM for 48 h. Images of the wounded area were photographed at 0 and 48 h after wounding under a light microscope (magnification, $\times 100$).

2.7 Transwell assay

Transwell assay was adopted to detect cell invasive capability. SK-N-SH cells were re-suspended in fresh serum-free DMEM and seeded at a density of 2×10^4 cells/well into the upper layer of transwell chamber precoated with matrigel. The complete medium was placed to the lower layer of transwell chamber as a chemoattractant. After 48 h incubation at 37 °C, non-invaded cells in the upper chambers were gently removed and invaded cells in the lower chambers were fixed with 4% paraformaldehyde, stained with 0.1% crystal violet and then photographed and quantitatively counted under a light microscope (magnification, $\times 200$).

2.8 Tube formation assay

HUVECs (2×10^4 cells/well) were seeded on 96-well plates precoated with Matrigel and then incubated with conditioned media of SK-N-SH cells for 24 h at 37 °C. Tube formation was observed and photographed under a light microscope (magnification, $\times 100$).

2.9 Western blot assay

Total protein was extracted using RIPA buffer containing protease inhibitors and centrifuged for 5 min at $12,000 \times g$ at 4 °C. BCA method was employed for protein quantification. Equal amount of protein samples were loaded and separated by sodium dodecyl sulphate–polyacrylamide gel electrophoresis (SDS-PAGE) and then electroblotted onto polyvinylidene fluoride (PVDF) membranes. After blocking with 5% bovine serum albumin (BSA) for 1 h at room temperature, membranes were incubated with primary antibodies against E-cadherin (Abcam, ab314063; 1:1000), N-cadherin (Abcam, ab76011; 1:5000), Snail (Abcam, ab216347; 1:1000), VE-cadherin (Abcam, ab314094; 1:1000), p-ERK (Abcam, ab201015; 1:1000), ERK (Abcam, ab216347; 1:10,000), VEGFA (Abcam, ab214424; 1:1000), MMP2 (Abcam, ab181286; 1:1000), MMP14 (Abcam, ab53712; 1:1000), MMP9 (Abcam, ab137867; 1:1000) and GAPDH (Abcam, ab9485; 1:2500) overnight at 4 °C. On the second day, membranes were incubated with horseradish peroxidase-conjugated secondary antibody (Abcam, ab205718, 1:50,000) for 1 h at room temperature. Protein signals were developed with electrochemiluminescence (ECL) detection kit (Beyotime, Shanghai, China) and the relative densities of individual bands were quantified using Image J software with GAPDH as the internal reference.

2.10 Molecular docking

The 3-D structure of ERK was obtained from protein the data bank (PDB) database (<https://www.rcsb.org/>). Molecular docking was carried out using AutoDockTools 4.2 software (<https://autodock.scripps.edu/>) and the 3D diagrams of molecular docking models were visualized by PyMol software (<https://pymol.org/>).

2.11 Biotin pull-down assay

Biotin pull-down assay was adopted to analyze the interaction between FKA and ERK by employing Pierce™ Biotinylated Protein Interaction Pull-Down Kit (Thermo Fisher Scientific, MA, USA). SK-N-SH cells were lysed in RIPA buffer containing protease inhibitors and the collected supernatants of cell lysates were incubated with biotin-FKA (10 μ M) or free biotin (10 μ M) for 12 h at 4 °C. Then, pre-cleaned streptavidin-conjugated agarose beads were added to the system above for additional 2 h incubation. After removing the supernatant and boiling the beads in SDS-PAGE sample buffer, the samples were tested by immunoblot for analysis.

2.12 Statistical analysis

Statistical analysis was performed using one-way analysis of variance (ANOVA) followed by Tukey's post hoc test. Data of three independent experiments were presented as mean values \pm SD. Statistically significant differences were set at $P < 0.05$.

3 Results

3.1 FKA treatment suppresses the proliferative and clone-forming abilities of NB cells

FKA is a novel chalcone isolated from the roots of the kava plant (Fig. 1A). Human NB cell line (SK-N-SH) and HUVECs were treated with 0, 12.5, 25, 50 μ M FKA for 48 h and cell viabilities were assessed using CCK-8 assay. FKA treatment had no obvious influence on the viability of HUVECs (Fig. 1B) while obviously reduced the viability of SK-N-SH cells in a

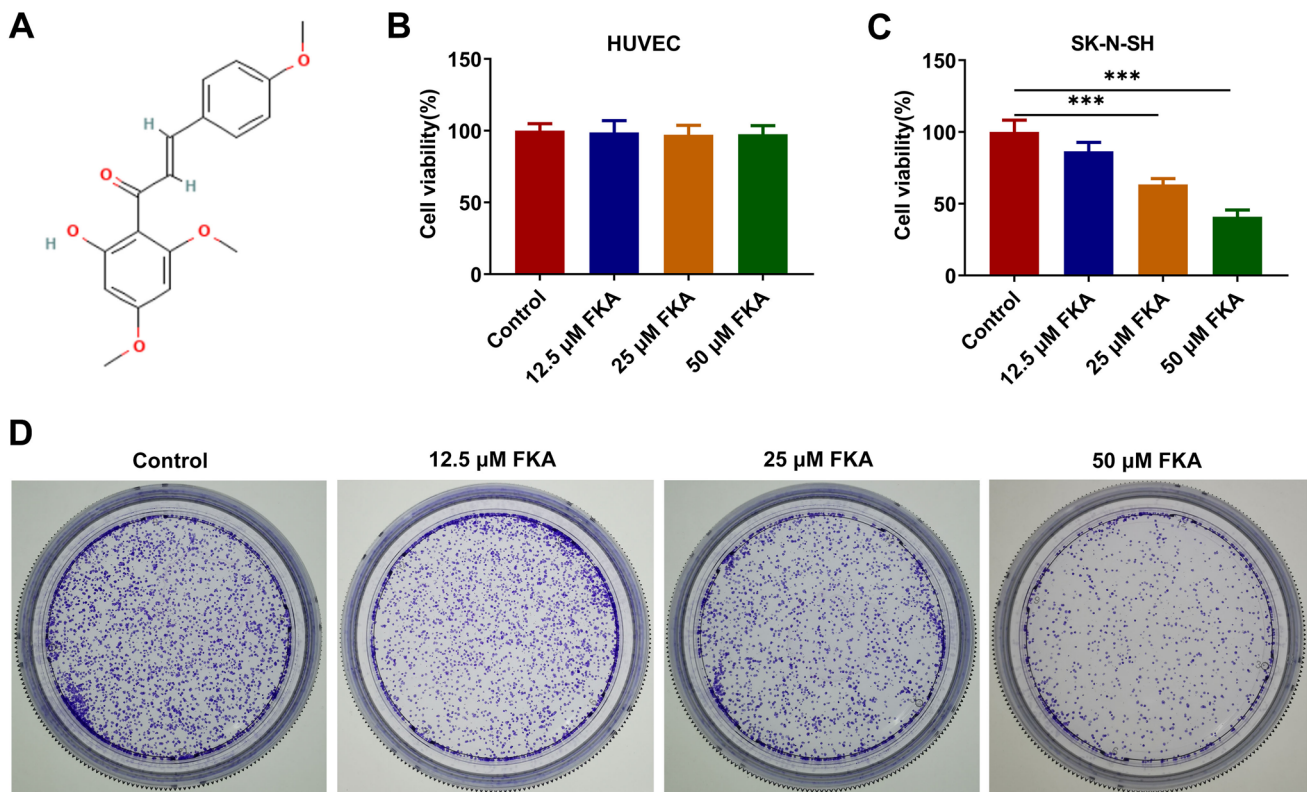


Fig. 1 FKA treatment suppresses the proliferative and clone-forming abilities of NB cells. **A** The structure of FKA. **B** HUVECs were treated with 0, 12.5, 25, 50 μ M FKA for 48 h. The viability of HUVECs was detected by CCK-8 assay. **C** Human NB cell line (SK-N-SH) was treated with 0, 12.5, 25, 50 μ M FKA for 48 h. The viability of SK-N-SH cells was detected by CCK-8 assay. **D** SK-N-SH cells were treated with 0, 12.5, 25, 50 μ M FKA for 48 h. The clone-forming ability of SK-N-SH cells was detected by colony formation assay. *** $p < 0.001$

dose-dependent manner (Fig. 1C). Meanwhile, colony formation assay revealed that FKA treatment also dose-dependently repressed the clone-forming ability of SK-N-SH cells (Fig. 1D).

3.2 FKA treatment facilitates NB cell apoptosis and arrests NB cell cycle

Flow cytometry analysis of cell apoptotic rate revealed that FKA treatment boosted the apoptosis of SK-N-SH cells in a dose-dependent manner (Fig. 2A). Besides, flow cytometry analysis of cell cycle distribution revealed that FKA treatment dose-dependently elevated the proportion of SK-N-SH cells at G1 phase and reduced the proportion of SK-N-SH cells at S phase, inducing NB cell cycle arrest (Fig. 2B).

3.3 FKA treatment inhibits NB cell migration, invasion and EMT

Cell migratory and invasive capabilities were assessed by employing wound healing and transwell assays. FKA treatment dose-dependently repressed the migration and invasion of SK-N-SH cells (Fig. 3A, B). Additionally, expressions of EMT-associated proteins were measured by western blot analysis. Increased expression of E-cadherin and decreased expressions of N-cadherin and Snail indicated that FKA treatment dose-dependently repressed EMT in NB (Fig. 3C).

3.4 FKA treatment represses in vitro angiogenesis

Angiogenesis is responsible for nutritional provision of tumor growth and metastasis [13]. HUVECs were incubated with the conditioned media of SK-N-SH cells treated with various concentrations (0, 12.5, 25, 50 μM) of FKA at 37 $^{\circ}\text{C}$ for 24 h. Tube formation assay for evaluating angiogenesis ability of HUVECs revealed that FKA treatment restrained in vitro angiogenesis in a dose-dependent manner (Fig. 4A). Concomitantly, VE-cadherin, the marker of angiogenesis, was measured by western blot analysis. Decreased expression of VE-cadherin also indicated that FKA treatment dose-dependently repressed in vitro angiogenesis of NB cells (Fig. 4B).

3.5 FKA targets on ERK to inactivate ERK/VEGF/MMPs signaling pathway

Molecular docking was carried out to explore the compound-protein binding potential between FKA and ERK and result demonstrated that FKA could interact with ERK at the sites of ARG:67, TYR:36, VAL:39, LEU:156 and ASN:154 (Fig. 5A). Furthermore, biotin pull-down assay confirmed the binding of FKA to ERK (Fig. 5B). ERK served as a downstream target of FKA. Afterward, ERK/VEGF/MMPs signaling pathway was examined by western blot analysis. FKA treatment dose-dependently

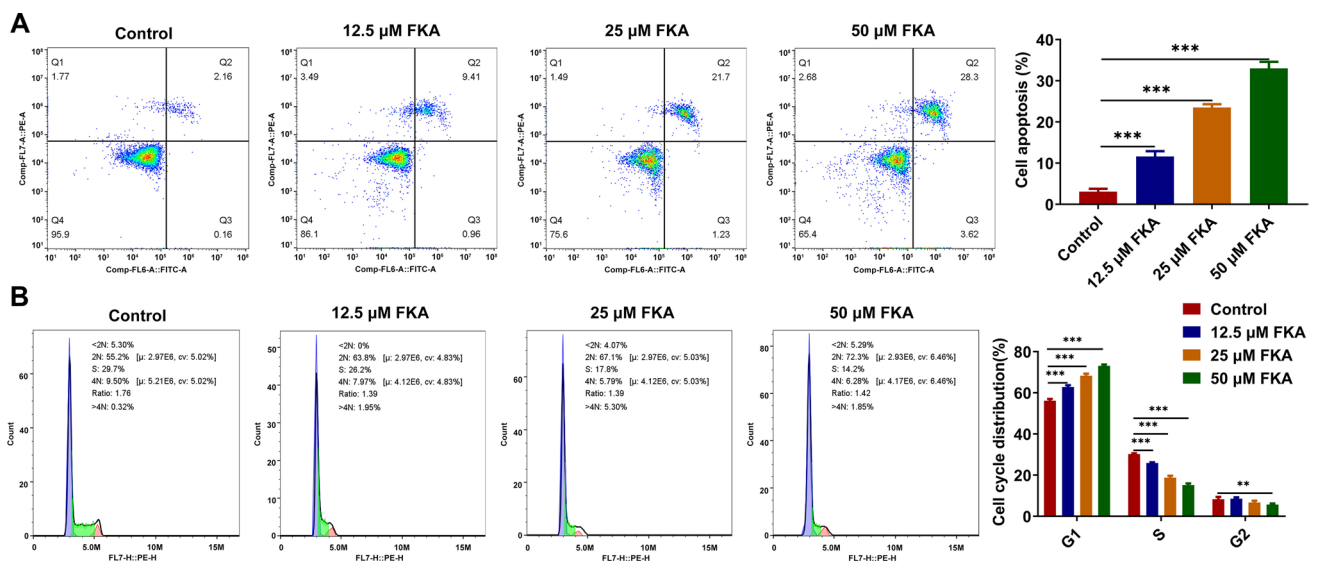


Fig. 2 FKA treatment facilitates NB cell apoptosis and arrests NB cell cycle. SK-N-SH cells were treated with 0, 12.5, 25, 50 μM FKA for 48 h. **A** The apoptotic rate of SK-N-SH cells was detected by flow cytometry analysis. **B** The cycle distribution of SK-N-SH cells was detected by flow cytometry analysis. ** $p < 0.01$, *** $p < 0.001$

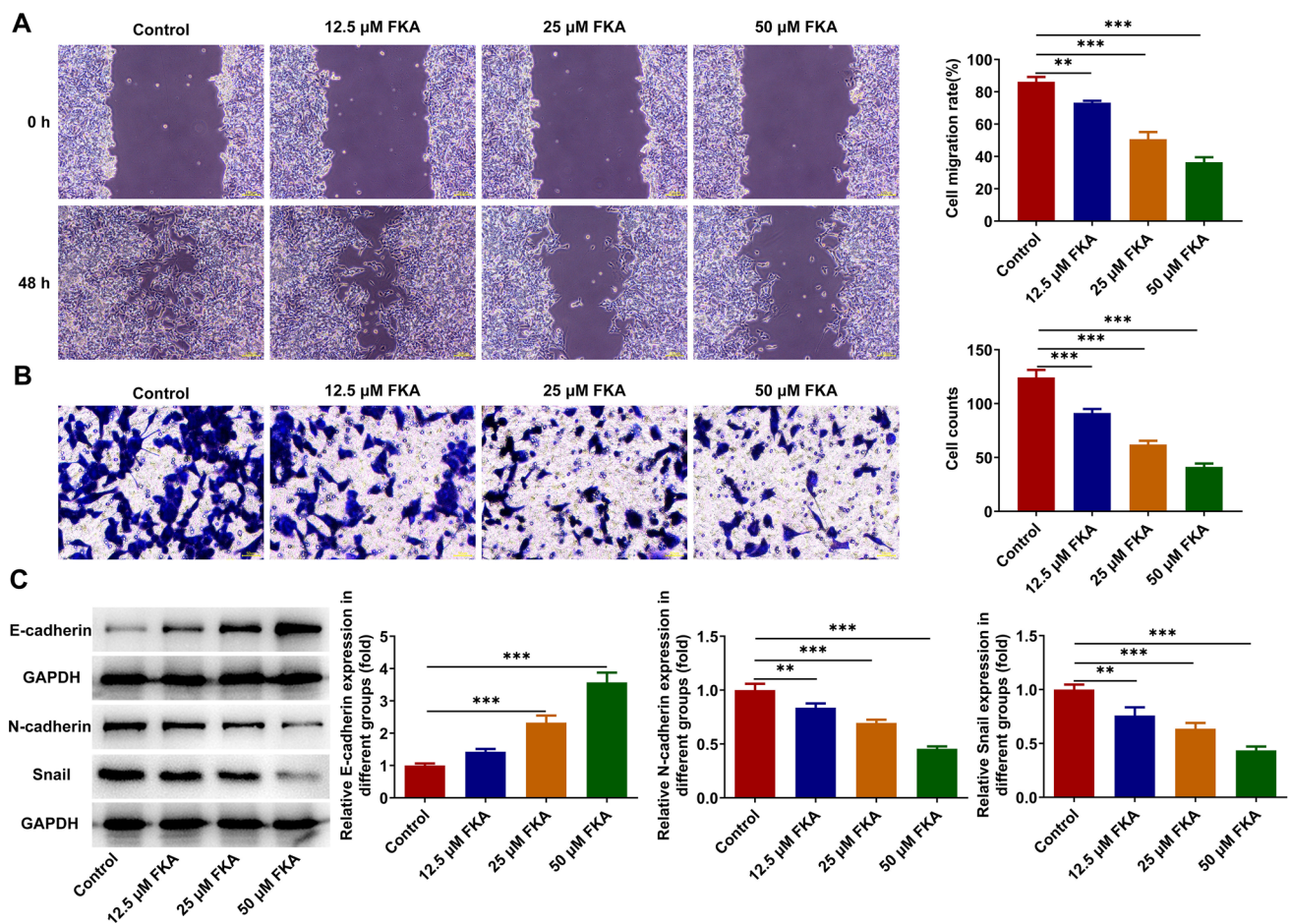


Fig. 3 FKA treatment inhibits NB cell migration, invasion and EMT. SK-N-SH cells were treated with 0, 12.5, 25, 50 μ M FKA for 48 h. **A** The migratory ability of SK-N-SH cells was detected by transwell assay. **B** The invasive ability of SK-N-SH cells was detected by transwell assay. **C** Expressions of E-cadherin, N-cadherin and Snail in SK-N-SH cells were detected by western blot analysis. ** $p < 0.01$, *** $p < 0.001$

inhibited the expressions of p-ERK, VEGFA, MMP2, MMP14 and MMP9, indicating that FKA could target on ERK and act as an inhibitor of ERK/VEGF/MMPs signaling pathway in NB (Fig. 5C).

3.6 FKA treatment suppresses NB cell growth, facilitates NB cell apoptosis and arrests NB cell cycle by inactivating ERK/VEGF/MMPs signaling pathway

To elucidate the intrinsic molecular mechanisms underlying the tumor-inhibiting functions of FKA in NB, SK-N-SH cells were treated with FKA for functional experiments and co-treated with ERK activator LM22B-10 for rescue experiments. FKA treatment reduced the viability and clone-forming ability of SK-N-SH cells, which were partially restored by LM22B-10 treatment (Fig. 6A, B). In addition, FKA treatment facilitated the apoptosis of SK-N-SH cells, which was partially reversed by LM22B-10 treatment (Fig. 6C). LM22B-10 treatment reduced the proportion of SK-N-SH cells at G1 phase and elevated the proportion of SK-N-SH cells at S phase, indicating that activation of ERK/VEGF/MMPs signaling pathway partially abolished the promoting effect of FKA on NB cell cycle arrest (Fig. 6D). To sum up, FKA treatment may suppress NB cell growth, facilitate NB cell apoptosis and arrest NB cell cycle depending on inactivation of ERK/VEGF/MMPs signaling pathway.

3.7 FKA treatment inhibits NB cell migration, invasion and EMT by inactivating ERK/VEGF/MMPs signaling pathway

FKA treatment repressed the migration and invasion of SK-N-SH cells, which were partially reversed by LM22B-10 treatment (Fig. 7A, B). Additionally, LM22B-10 treatment decreased expression of E-cadherin and increased expressions of

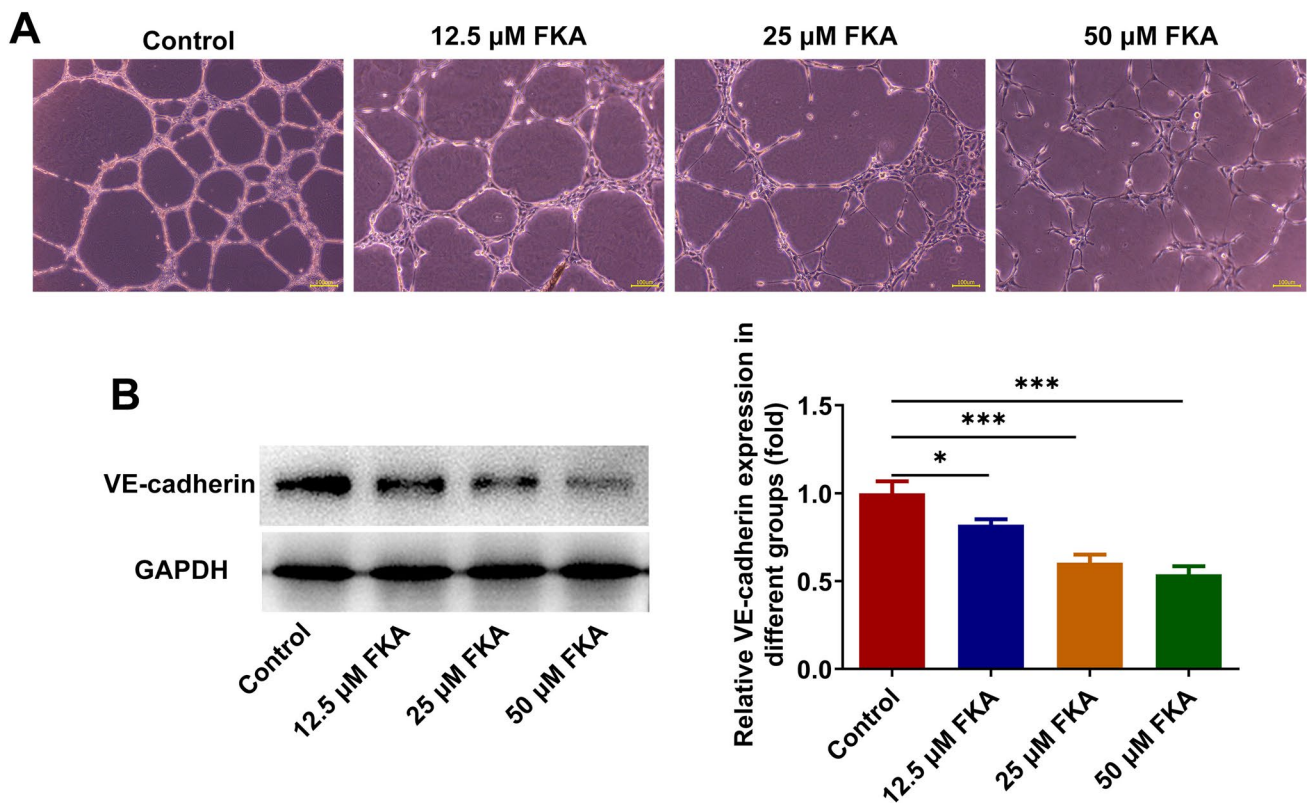


Fig. 4 FKA treatment represses in vitro angiogenesis. **A** HUVECs were incubated with the conditioned media of SK-N-SH cells treated with various concentrations (0, 12.5, 25, 50 μM) of FKA at 37 °C for 24 h. In vitro angiogenesis of HUVECs was detected by tube formation assay. **B** SK-N-SH cells were treated with 0, 12.5, 25, 50 μM FKA for 48 h. Expression of VE-cadherin in SK-N-SH cells was detected by western blot analysis. * $p < 0.05$, *** $p < 0.001$

N-cadherin and Snail, indicating that activation of ERK/VEGF/MMPs signaling pathway partially abolished the suppressing effect of FKA on EMT in NB (Fig. 7C). To conclude, FKA treatment may inhibit NB cell migration, invasion and EMT depending on inactivation of ERK/VEGF/MMPs signaling pathway.

3.8 FKA treatment represses in vitro angiogenesis by inactivating ERK/VEGF/MMPs signaling pathway

HUVECs were incubated with the conditioned media of SK-N-SH cells treated with FKA or co-treated with FKA and ERK activator LM22B-10 at 37 °C for 24 h. LM22B-10 treatment strengthened tube formation ability of HUVECs and increased expression of VE-cadherin, indicating that activation of ERK/VEGF/MMPs signaling pathway partially abolished the inhibiting effect of FKA on in vitro angiogenesis of NB cells (Fig. 8A, B). In a word, FKA treatment may repress in vitro angiogenesis depending on inactivation of ERK/VEGF/MMPs signaling pathway.

4 Discussion

NB, a lethal cancer of the brain, is the most common extracranial solid tumor in children with poor prognosis and low survival rate owing to high recurrence rate, strong invasiveness and high metastasis rate [14]. Currently, conventional therapies such as chemotherapy followed by autologous stem cell transplant, surgery, radiotherapy and immunotherapy are frequently associated with severe side effects. Hence, screening for specific and sensitive tumor biomarkers or efficacious therapeutic options are of great urgency. The present study addressed the anticarcinogenic effects of FKA against the malignant behaviors of NB cells and thoroughly elucidated the intrinsic molecular mechanisms underlying the tumor-inhibiting functions of FKA in NB.

In our current work, it was verified that FKA treatment suppressed the proliferative and clone-forming abilities of NB cells, facilitated NB cell apoptosis, arrested NB cell cycle as well as inhibited NB cell migration, invasion, EMT

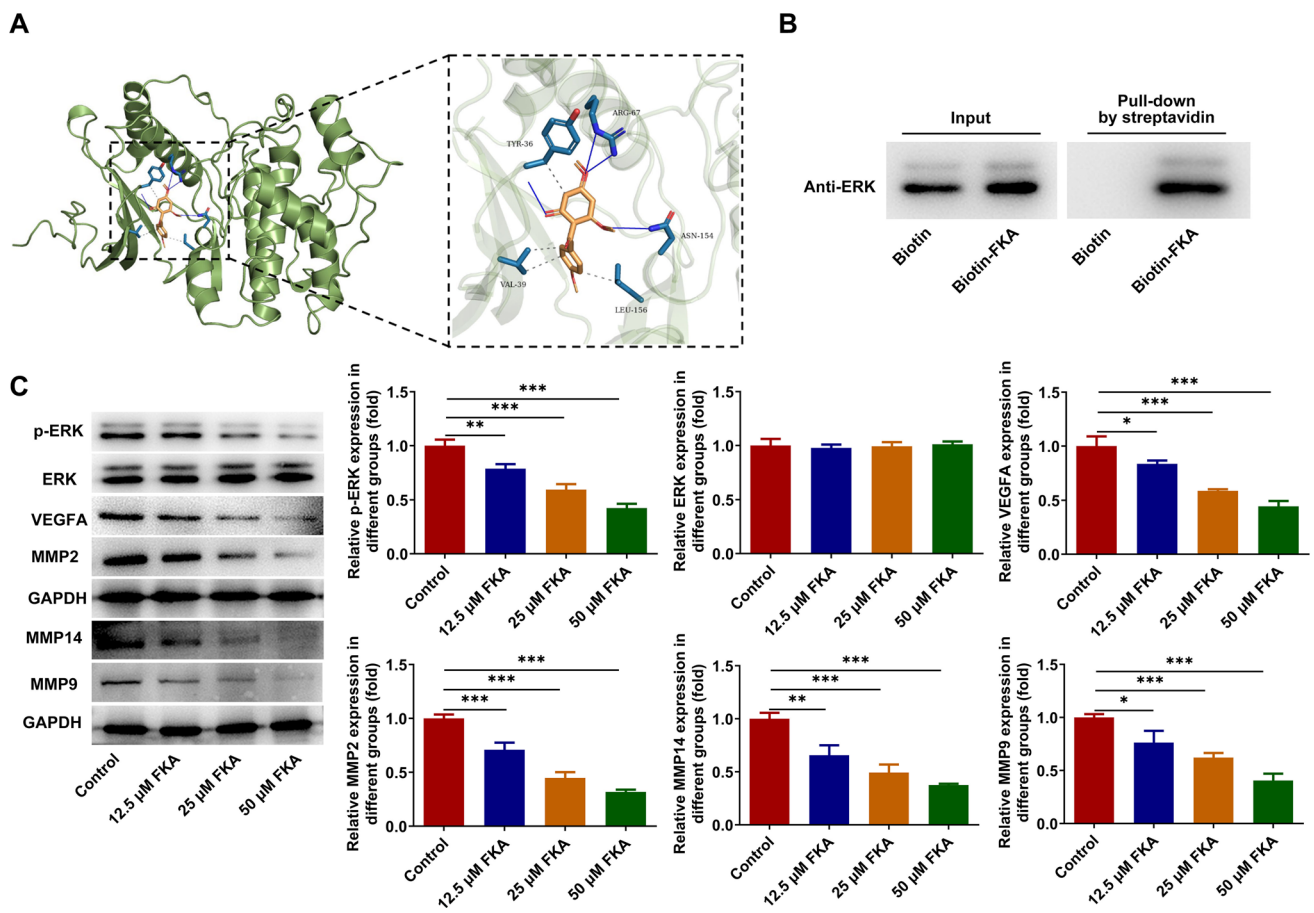


Fig. 5 FKA targets on ERK to inactivate ERK/VEGF/MMPs signaling pathway. **A** Molecular docking of the compound-protein interaction between FKA and ERK. **B** The binding of FKA to ERK was validated by biotin pull-down assay. **C** SK-N-SH cells were treated with 0, 12.5, 25, 50 μM FKA for 48 h. Expressions of p-ERK, ERK, VEGFA, MMP2, MMP14 and MMP9 in SK-N-SH cells were detected by western blot analysis. * $p < 0.05$, ** $p < 0.01$, *** $p < 0.001$

and in vitro angiogenesis in a dose-dependent manner. What's more, molecular docking predicted the compound-protein interaction between FKA and ERK and biotin pull-down assay validated the binding of FKA to ERK. Our work verified that FKA targeted on ERK to inactivate ERK/VEGF/MMPs signaling pathway.

Extracellular signal-regulated kinases (ERK) are members of mitogen-activated protein kinase (MAPK) super family [15]. Activated via phosphorylation, ERK transduces extracellular signal into nucleus to trigger expression and transcription responses [16]. ERK is involved in a series of cellular processes, including cell proliferation, differentiation, survival and death [17]. It has been well documented that ERK is closely associated with tumor growth and metastasis and ERK has been widely accepted as a key target in the diagnosis and treatment of cancers [18]. In human cancer models, ERK inhibition exhibits potent antiangiogenic effects with decreased VEGF expression and signaling [19, 20], suggesting that ERK plays an important role in regulation of angiogenesis in cancers via mediating VEGF. Besides, ERK signaling promotes tumor growth, angiogenesis and metastasis also by mediating MMPs pathway [21–23]. Literature reports that miR-429 deficiency negatively correlated with CRKL overexpression promotes clear cell renal cell carcinoma malignant progression through activating SOS1/MEK/ERK/MMP2/MMP9 pathway [24]. Propofol suppresses proliferation, invasion and angiogenesis of esophageal squamous cell carcinoma cells by inactivating ERK/VEGF/MMP-9 signaling [25]. WNT5A promotes migration and invasion of human osteosarcoma

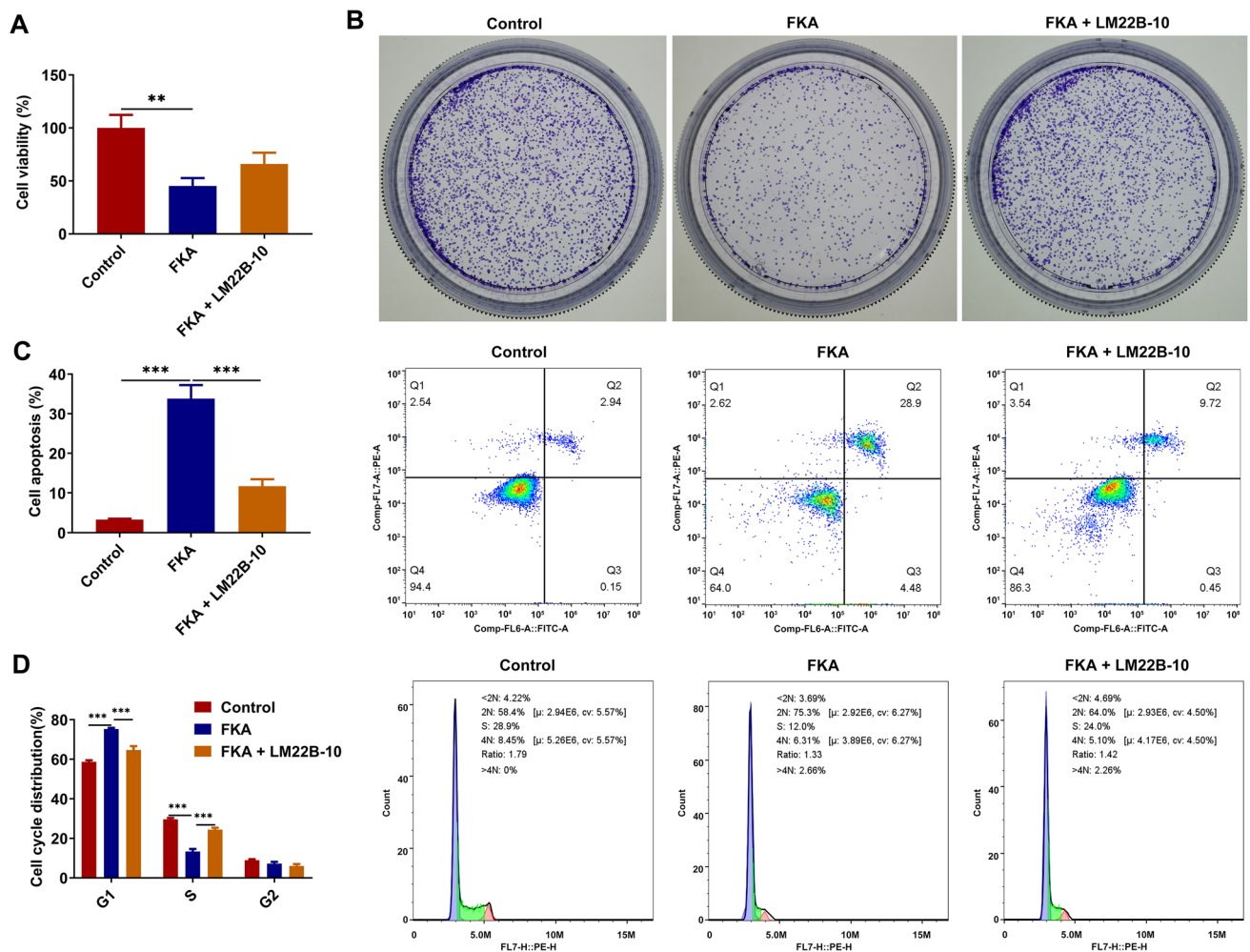


Fig. 6 FKA treatment suppresses NB cell growth, facilitates NB cell apoptosis and arrests NB cell cycle by inactivating ERK/VEGF/MMPs signaling pathway. SK-N-SH cells were treated with FKA or co-treated with FKA and ERK activator LM22B-10. **A** The viability of SK-N-SH cells was detected by CCK-8 assay. **B** The clone-forming ability of SK-N-SH cells was detected by colony formation assay. **C** The apoptotic rate of SK-N-SH cells was detected by flow cytometry analysis. **D** The cycle distribution of SK-N-SH cells was detected by flow cytometry analysis. $**p < 0.01$, $***p < 0.001$

cells via activating SRC/ERK/MMP-14 pathway [26]. In our current work, it was verified that LM22B-10 treatment facilitated NB cell growth as well as suppressed the apoptosis, cell cycle arrest, migration, invasion, EMT and in vitro angiogenesis of NB cells, partially abolishing the tumor-inhibiting functions of FKA in NB.

5 Conclusion

To conclude, FKA may suppress the malignant behaviors of NB cells depending on inactivation of ERK/VEGF/MMPs signaling pathway. FKA can act as an anti-tumorigenic drug in NB though suppression of ERK/VEGF/MMPs signaling. Findings are beneficial to the development of promising agents and effective therapeutic targets for NB. In spite of the aforementioned achievement, the current study appears to have limitations due to the lack of in vivo experiments. In future studies, in vivo animal experiments should be carried out to enhance the persuasiveness of the conclusions in the present research and to excavate the predictive values of FKA in NB therapies clinically.

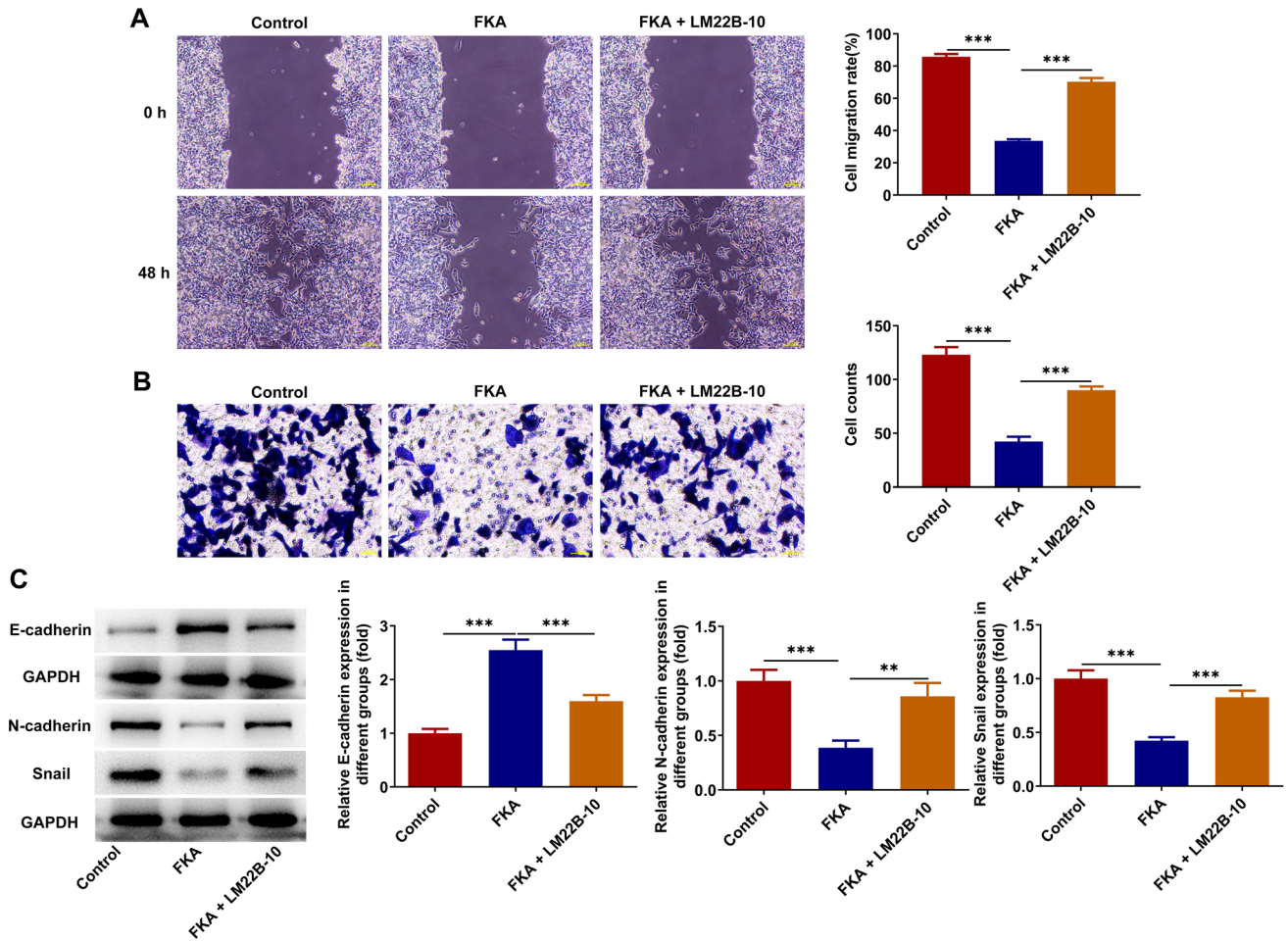
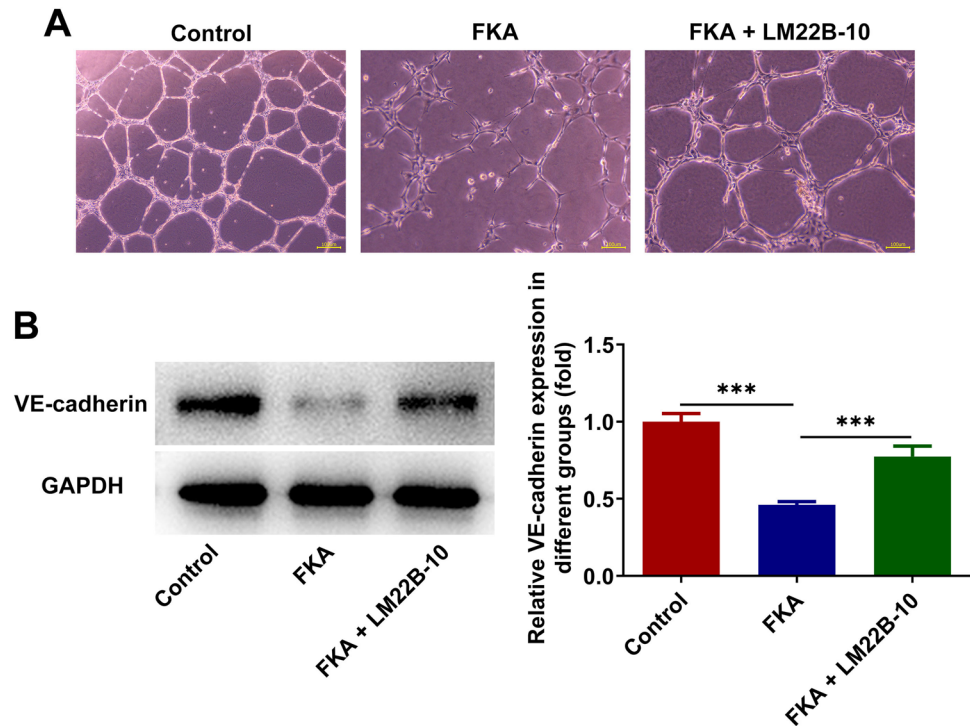


Fig. 7 FKA treatment inhibits NB cell migration, invasion and EMT by inactivating ERK/VEGF/MMPs signaling pathway. SK-N-SH cells were treated with FKA or co-treated with FKA and ERK activator LM22B-10. **A** The migratory ability of SK-N-SH cells was detected by wound healing assay. **B** The invasive ability of SK-N-SH cells was detected by transwell assay. **C** Expressions of E-cadherin, N-cadherin and Snail in SK-N-SH cells were detected by western blot analysis. $**p < 0.01$, $***p < 0.001$

Fig. 8 FKA treatment represses in vitro angiogenesis by inactivating ERK/VEGF/MMPs signaling pathway. **A** HUVECs were incubated with the conditioned media of SK-N-SH cells treated with FKA or co-treated with FKA and ERK activator LM22B-10 at 37 °C for 24 h. In vitro angiogenesis of HUVECs was detected by tube formation assay. **B** SK-N-SH cells were treated with FKA or co-treated with FKA and ERK activator LM22B-10. Expression of VE-cadherin in SK-N-SH cells was detected by western blot analysis. *** $p < 0.001$



Acknowledgements None.

Author contributions Mengyao Dong contributed to the conception, study design, experimental operation, data analysis, paper writing and critical revision. Gaiqin Li contributed to the study design, experimental operation, data collection, data analysis and paper writing. Geng Geng contributed to the study design, experimental operation, data analysis and paper writing. Ming Ming contributed to the experimental operation, data collection, data analysis and paper writing. Yongtao Xu contributed to the conception, study design, paper writing and critical revision. All authors read and approved the final manuscript for publication.

Funding None.

Data availability The datasets used and/or analyzed during the present study are available from the corresponding author on reasonable request.

Declarations

Ethics approval and consent to participate Not applicable.

Competing interests The authors declare no competing interests.

Open Access This article is licensed under a Creative Commons Attribution-NonCommercial-NoDerivatives 4.0 International License, which permits any non-commercial use, sharing, distribution and reproduction in any medium or format, as long as you give appropriate credit to the original author(s) and the source, provide a link to the Creative Commons licence, and indicate if you modified the licensed material. You do not have permission under this licence to share adapted material derived from this article or parts of it. The images or other third party material in this article are included in the article's Creative Commons licence, unless indicated otherwise in a credit line to the material. If material is not included in the article's Creative Commons licence and your intended use is not permitted by statutory regulation or exceeds the permitted use, you will need to obtain permission directly from the copyright holder. To view a copy of this licence, visit <http://creativecommons.org/licenses/by-nc-nd/4.0/>.

References

1. Wang H, Shi B, Zhang X, Shen P, He Q, Yin M, et al. Exosomal hsa-piR1089 promotes proliferation and migration in neuroblastoma via targeting KEAP1. *Pathol Res Pract*. 2023;241: 154240. <https://doi.org/10.1016/j.prp.2022.154240>.
2. Geroges A. Canning U neuroblastoma and its target therapies: a medicinal chemistry review. *ChemMedChem*. 2024;19: e202300535. <https://doi.org/10.1002/cmdc.202300535>.

3. Suo C, Deng W, Vu TN, Li M, Shi L, Pawitan Y Accumulation of potential driver genes with genomic alterations predicts survival of high-risk neuroblastoma patients. *Biol Direct.* 2018;13:14. <https://doi.org/10.1186/s13062-018-0218-5>.
4. Abu N, Ho WY, Yeap SK, Akhtar MN, Abdullah MP, Omar AR, et al. The flavokawains: uprising medicinal chalcones. *Cancer Cell Int.* 2013;13:102. <https://doi.org/10.1186/1475-2867-13-102>.
5. Liu S, Liu Z, Piao C, Zhang Z, Kong C, Yin L, et al. Flavokawain A is a natural inhibitor of PRMT5 in bladder cancer. *J Exp Clin Cancer Res.* 2022;41:293. <https://doi.org/10.1186/s13046-022-02500-4>.
6. Song L, Mino M, Yamak J, Nguyen V, Lopez D, Pham V, et al. Flavokawain A reduces tumor-initiating properties and stemness of prostate cancer. *Front Oncol.* 2022;12: 943846. <https://doi.org/10.3389/fonc.2022.943846>.
7. Li J, Zheng L, Yan M, Wu J, Liu Y, Tian X, et al. Activity and mechanism of flavokawain A in inhibiting P-glycoprotein expression in paclitaxel resistance of lung cancer. *Oncol Lett.* 2020;19:379–87. <https://doi.org/10.3892/ol.2019.11069>.
8. Zhang M, Xue J, Chen X, Elsaid FG, Salem ET, Ghanem RA, et al. Bioactivity of hamamelitannin, flavokawain A, and triacetyl resveratrol as natural compounds: Molecular docking study, anticolon cancer, and anti-Alzheimer potentials. *Biotechnol Appl Biochem.* 2023;70:730–45. <https://doi.org/10.1002/bab.2394>.
9. Abu N, Akhtar MN, Yeap SK, Lim KL, Ho WY, Zulfadli AJ, et al. Flavokawain A induces apoptosis in MCF-7 and MDA-MB231 and inhibits the metastatic process in vitro. *PLoS ONE.* 2014;9: e105244. <https://doi.org/10.1371/journal.pone.0105244>.
10. Xiao T, Bao J, Tian J, Lin R, Zhang Z, Zhu Y, et al. Flavokawain A suppresses the vasculogenic mimicry of HCC by inhibiting CXCL12 mediated EMT. *Phytomedicine.* 2023;112: 154687. <https://doi.org/10.1016/j.phymed.2023.154687>.
11. Wang K, Zhang W, Wang Z, Gao M, Wang X, Han W, et al. Flavokawain A inhibits prostate cancer cells by inducing cell cycle arrest and cell apoptosis and regulating the glutamine metabolism pathway. *J Pharm Biomed Anal.* 2020;186: 113288. <https://doi.org/10.1016/j.jpba.2020.113288>.
12. Xu Y, Ma Y, Liu XL, Gao SL miR-133b affects cell proliferation, invasion and chemosensitivity in renal cell carcinoma by inhibiting the ERK signaling pathway. *Mol Med Rep.* 2020;22:67–76. <https://doi.org/10.3892/mmr.2020.11125>.
13. Paduch R. The role of lymphangiogenesis and angiogenesis in tumor metastasis. *Cell Oncol (Dordr).* 2016;39:397–410. <https://doi.org/10.1007/s13402-016-0281-9>.
14. Katta SS, Nagati V, Paturi ASV, Murakonda SP, Murakonda AB, Pandey MK, et al. Neuroblastoma: emerging trends in pathogenesis, diagnosis, and therapeutic targets. *J Control Release.* 2023;357:444–59. <https://doi.org/10.1016/j.jconrel.2023.04.001>.
15. Johnson GL, Lapadat R. Mitogen-activated protein kinase pathways mediated by ERK, JNK, and p38 protein kinases. *Science.* 2002;298:1911–2. <https://doi.org/10.1126/science.1072682>.
16. Patel AL, Shvartsman SY. Outstanding questions in developmental ERK signaling. *Development.* 2018. <https://doi.org/10.1242/dev.143818>.
17. Deschenes-Simard X, Malleshaiah M, Ferbeyre G. Extracellular signal-regulated kinases: one pathway, multiple fates. *Cancers (Basel).* 2023. <https://doi.org/10.3390/cancers16010095>.
18. Sugiura R, Satoh R, Takasaki T. ERK: A Double-Edged Sword in Cancer. ERK-dependent apoptosis as a potential therapeutic strategy for cancer. *Cells.* 2021. <https://doi.org/10.3390/cells10102509>.
19. Wang Z, Zhao P, Tian K, Qiao Z, Dong H, Li J, et al. TMEM9 promotes lung adenocarcinoma progression via activating the MEK/ERK/STAT3 pathway to induce VEGF expression. *Cell Death Dis.* 2024;15:295. <https://doi.org/10.1038/s41419-024-06669-8>.
20. Huang CL, Achudhan D, Liu PI, Lin YY, Liu SC, Guo JH, et al. Visfatin upregulates VEGF-C expression and lymphangiogenesis in esophageal cancer by activating MEK1/2-ERK and NF-kappaB signaling. *Aging.* 2023;15:4774–93. <https://doi.org/10.18632/aging.204762>.
21. Zhang JG, Zhang DD, Liu Y, Hu JN, Zhang X, Li L, et al. RhoC/ROCK2 promotes vasculogenic mimicry formation primarily through ERK/MMPs in hepatocellular carcinoma. *Biochim Biophys Acta, Mol Basis Dis.* 2019;1865:1113–25. <https://doi.org/10.1016/j.bbadis.2018.12.007>.
22. Zhao Y, Hu F, Wang Q. Cortactin contributes to the tumorigenesis of gastric cancer by activating ERK/MMP pathway. *Heliyon.* 2023;9: e18289. <https://doi.org/10.1016/j.heliyon.2023.e18289>.
23. Wang M, Huang C, Gao W, Zhu Y, Zhang F, Li Z, et al. MicroRNA-181a-5p prevents the progression of esophageal squamous cell carcinoma in vivo and in vitro via the MEK1-mediated ERK-MMP signaling pathway. *Aging.* 2022;14:3540–53. <https://doi.org/10.18632/aging.204028>.
24. Wang J, Wang C, Li Q, Guo C, Sun W, Zhao D, et al. miR-429-CRKL axis regulates clear cell renal cell carcinoma malignant progression through SOS1/MEK/ERK/MMP2/MMP9 pathway. *Biomed Pharmacother.* 2020;127: 110215. <https://doi.org/10.1016/j.biopha.2020.110215>.
25. Xu YB, Du QH, Zhang MY, Yun P. He CY Propofol suppresses proliferation, invasion and angiogenesis by down-regulating ERK-VEGF/MMP-9 signaling in Eca-109 esophageal squamous cell carcinoma cells. *Eur Rev Med Pharmacol Sci.* 2013;17:2486–94.
26. Wang X, Zhao X, Yi Z, Ma B, Wang H, Pu Y, et al. WNT5A promotes migration and invasion of human osteosarcoma cells via SRC/ERK/MMP-14 pathway. *Cell Biol Int.* 2018;42:598–607. <https://doi.org/10.1002/cbin.10936>.

Publisher's Note Springer Nature remains neutral with regard to jurisdictional claims in published maps and institutional affiliations.